Preparation and Characterization of $Cs_{2.8}H_{1.2}PMo_{11}Fe(H_2O)O_{39}\cdot 6H_2O$ and Investigation of Effects of Iron-Substitution on Heterogeneous Oxidative Dehydrogenation of 2-Propanol

Noritaka Mizuno,* Joon-Seok Min, and Akira Taguchi

Department of Applied Chemistry, School of Engineering, The University of Tokyo, 7-3-1 Hongo, Bunkyo-ku, Tokyo 113-8656, Japan

Received September 23, 2003. Revised Manuscript Received May 11, 2004

Synthesis and characterization of mono-iron(III)-substituted molybdophosphate, the solidification as a heterogeneous catalyst, and the oxidative dehydrogenation of 2-propanol were reported. The catalyst was isolated as $Cs_{2.8}H_{1.2}PMo_{11}Fe(H_2O)O_{39}\cdot 6H_2O$, and characterized by elemental analysis and X-ray diffraction, infrared, ^{31}P NMR, and ESR spectroscopy. The Fe^{3+} in $Cs_{2.8}H_{1.2}PMo_{11}Fe(H_2O)O_{39}\cdot 6H_2O$ was incorporated into the molybdophosphate framework while that in Fe^{3+}(2.5 wt %)/$Cs_{3.0}PMo_{12}O_{40}$ existed as a countercation in a relatively distorted octahedral site. The seven water molecules were desorbed by the thermal treatment at 63 °C and the cesium hydrogen salt was stable below 210 °C. The cesium hydrogen salt was used for heterogeneous oxidative dehydrogenation of 2-propanol to acetone and intrinsically has a higher rate than those for the iron-impregnated $Fe^{3+}/Cs_{3.0}PMo_{12}O_{40}$ and $Cs_{3.0}PMo_{12}O_{40}$ catalysts, showing the effectiveness of isolated iron in the $PMo_{11}O_{39}^{7-}$ polyoxometalate on the oxidative dehydrogenation. The data for the stop of the supply of the oxygen at the stationary state in the flow experiment showed that acetone was produced by the reaction of 2-propanol with the cesium hydrogen salt. The correlation between intrinsic rates of oxidative dehydrogenation of 2-propanol and reducibility of catalysts, the rate equation of $-d[\text{2-PrOH}]/dt = k\cdot P_{2-\text{PrOH}}{}^{0.80}\cdot PO_2{}^{-0.06}$, and kinetic isotope effects of 1.6−1.9 showed that the reduction of the catalyst with the β-hydrogen elimination from 2-propanol was the rate-determining step.

Introduction

Understanding of heterogeneous catalysis has progressed much recently, and the control of active sites at atomic/molecular levels has been attempted with novel methods or modification of traditional techniques of precipitation, impregnation, and ion exchange. On this standpoint, the design and synthesis of heterogeneous catalysts and the demonstration of a remarkable effect on catalysis are very important.[1−5] Supported oxides, mixed oxides, framework-substituted molecular sieves/polyoxometalates, and heterogenized homogeneous catalysts have been used for the design of heterogeneous catalysts.

Catalytic function of heteropoly compounds in solid states has attracted much attention because the redox and acidic properties can be controlled at atomic/molecular levels by changing the constituent elements. Catalysis by α-Keggin-type polyoxometalates has most extensively been investigated because of their rather high thermal stability and ease of synthesis.[6−12] It has been reported that heteropoly compounds can catalyze oxidation of light alkanes[13−18] and that the catalytic performance is much enhanced by the addition of transition metals.[17−23]

* To whom correspondence should be addressed. E-mail: tmizuno@mail.ecc.u-tokyo.ac.jp.

(1) Corma, A. *Chem. Rev.* **1995**, *95*, 559.
(2) Carrier, X.; Lambert, J. F.; Che, M. *J. Am. Chem. Soc.* **1997**, *119*, 10137.
(3) Hutchings, G. J. *Chem. Commun.* **1999**, 301.
(4) Raja, R.; Sanker, G.; Thomas, J. M. *Angew. Chem., Int. Ed.* **2000**, *39*, 2313.
(5) Centi, G., Wichterlova, B., Bell, A. T., Eds. *Catalysis by Unique Metal Ion Structure in Solid Matrixes From Science to Application*; Kluwer Academic: Dordrecht, The Netherlands, 2001.
(6) Misono, M. *Catal. Rev. Sci. Eng.* **1987**, *29*, 269.
(7) Pope, M. T.; Müller, A. *Angew. Chem., Int. Ed. Engl.* **1991**, *30*, 34.
(8) Ono, Y. In *Perspectives in Catalysis;* Thomas, J. M., Zamaraev, K. I., Eds.; Blackwell: London, 1992; p 431.
(9) Kozhevnikov, I. V. *Catal. Rev. Sci. Eng.* **1995**, *37*, 311.
(10) Okuhara, T.; Mizuno, N.; Misono, M. *Adv. Catal.* **1996**, *41*, 113.
(11) Mizuno, N.; Misono, M. *Chem. Rev.* **1998**, *98*, 199.
(12) Kozhevnikov, I. V. *Chem. Rev.* **1998**, *98*, 171.
(13) Eguchi, K.; Aso, I.; Yamazoe, N.; Seiyama, T. *Chem. Lett.* **1979**, 1345.
(14) Niiyama, H.; Tsuneki, H.; Echigoya, E. *Nippon Kagaku Kaishi* **1979**, 996.
(15) Akimoto, M.; Tsuchida, Y.; Sato, K.; Echigoya, E. *J. Catal.* **1981**, *72*, 83.
(16) Ai, M. *Appl. Catal.* **1982**, *4*, 245.
(17) Min, J.-S.; Mizuno, N. *Catal. Today* **2001**, *66*, 47.
(18) Min, J.-S.; Ishige, H.; Misono, M.; Mizuno, N. *J. Catal.* **2001**, *198*, 116.
(19) Centi, G.; Nieto, J. L.; Iapalucci, C.; Brückman, K.; Serwicka, E. M. *Appl. Catal.* **1989**, *46*, 197.
(20) Centi, G.; Lena, V.; Trifirò, F.; Ghoussoub, D.; Aïssi, C. F.; Guelton, M.; Bonnelle, J. P. *J. Chem. Soc., Faraday Trans.* **1990**, *86*, 2775.
(21) Mizuno, N.; Tateishi, M.; Iwamoto, M. *Chem. Commun.* **1994**, 1411.
(22) Mizuno, N.; Tateishi, M.; Iwamoto, M. *J. Catal.* **1996**, *163*, 87.

10.1021/cm0348996 CCC: $27.50 © 2004 American Chemical Society
Published on Web 06/19/2004

Iron has often been used as an additive or component for redox catalysts in several inorganic, organic, and biological systems.[24−28] For example, incorporation of iron into the scheelite structure reduces the activation energy of reoxidation and promotes the exchange of oxygen between the bulk and the surface,[24] and oxidation of benzene to phenol has been industrialized by iron-containing ZSM-5 zeolite.[27] The addition of iron enhanced the catalytic performance of cesium hydrogen salts of molybdophosphates for selective oxidation of light alkanes under oxygen-rich and -poor conditions. The enhancement of the catalytic performance for the selective oxidation is attributed to the promotion of hydrogen abstraction from alkanes by the oxide ion (O^{2-}) neighboring Mo^{6+} in $PMo_{12}O_{40}^{3-}$.[21−23,29,30] It has been reported that transition metals incorporated into polyoxotungstates play significant roles as electron reservoirs or active sites for the activation of hydrocarbons and molecular oxygen.[7,10,12,31−33] Molybdenum-based oxides can catalyze various selective oxidation reactions in heterogeneous systems, and therefore it is expected that the incorporation of Fe^{3+} into the polyoxometalate framework results in enhancement of the catalytic performance.

During the past decade, there has been a great interest in synthesis and oxidation catalysis of transition-metal-substituted polyoxometalates due to their unique and remarkable influence on catalytic performances.[7,10,30,33,34] However, little is known of the oxidation catalysis by iron-substituted molybdophosphates because there are no reliable, reproducible, selective methods of their syntheses.[35−37] We have preliminarily reported the enhancement of the catalytic activity for the oxidative dehydrogenation of 2-propanol to acetone by the iron substitution for 12-molybdophosphate.[38]

In this work, we report full details of the preparation and characterization of $Cs_{2.8}H_{1.2}PMo_{11}Fe(H_2O)O_{39}\cdot 6H_2O$ and attempt to investigate the effects of iron on the catalytic activity for the oxidative dehydrogenation of 2-propanol.

Experimental Section

Materials. 12-Molybdophosphoric acid ($H_3PMo_{12}O_{40}\cdot 28H_2O$) was commercially obtained from Nippon Inorganic Color and Chemical Co., Ltd. and recrystallized from diethyl ether. Elemental analysis: found (calcd) P, 1.30 (1.33); Mo, 49.53 (49.42). The purity was confirmed by the ^{31}P NMR spectrum to be more than 98%. The other reagents were commercially obtained and used as received.

Preparation of Solid Catalysts. The cesium hydrogen salt of mono-iron-substituted phosphoundecamolybdate was synthesized as follows. $H_3PMo_{12}O_{40}\cdot 28H_2O$ (2.0 mmol) was dissolved in water (0.1 mol·dm^{-3}), and the pH of the solution was adjusted to 4.3 with lithium carbonate. Only one signal was observed at −0.9 ppm (vs 85% H_3PO_4) for the ^{31}P NMR spectrum, showing the presence of highly pure lacunary species, $PMo_{11}O_{39}^{7-}$. Then, ferric nitrate ($Fe(NO_3)_3\cdot 9H_2O$, 2.2 mmol) was added to the solution and the solution was filtered. To the reddish yellow filtrate was added cesium chloride (6.0 mmol) to yield a yellow precipitate. The precipitate was filtered off, washed with water, and aspirated to dryness (yield 55%, yellow). No chloride ions were detected for the precipitate by X-ray photoelectron spectroscopy and X-ray fluorometry. The TG/DTA profile of the precipitate showed an endothermic peak at 63 °C with a weight loss of 5.6 wt %, assignable to desorption of 7.0 water molecules/anion. Elemental analysis: found Cs, 16.43; P, 1.34; Mo, 46.37; Fe, 2.03%. Calcd for $Cs_{2.8}H_{1.2}[PMo_{11}\{Fe(H_2O)\}O_{39}]\cdot 6H_2O$: Cs, 16.43; P, 1.37; Mo, 46.58; Fe, 2.46%. Fe^{2+} could not be incorporated into $PMo_{11}O_{39}^{7-}$ in mixed solvents of acetonitrile, toluene, and water probably because of the lower ligating ability than Fe^{3+} or easier reduction of Mo^{6+}.[35,39]

More characterization was carried out for the phenyltrimethylammonium salt because $Cs_{2.8}H_{1.2}[PMo_{11}\{Fe(H_2O)\}O_{39}]\cdot 6H_2O$ was insoluble in any solvents without the decomposition of the anion structure. The phenyltrimethylammonium salt was crystallized in the triclinic space group $P\bar{1}$ with cell parameters of $a = 15.103(5)$ Å, $b = 20.708(5)$ Å, $c = 14.834(6)$ Å, $\alpha = 100.20(3)°$, $\beta = 116.55(2)°$, and $\gamma = 81.07(3)°$. The crystallographic data show that no iron ions are present as countercations. Elemental analysis: found C, 22.05; H, 2.96; N, 3.52; P, 1.20; Mo, 41.50; Fe, 2.15; Cl, 1.35%. Calcd for $[C_6H_5(CH_3)_3N]_5[PMo_{11}\{Fe(Cl)\}O_{39}]\cdot CH_3CN\cdot H_2O$: C, 22.21; H, 2.98; N, 3.31; P, 1.22; Mo, 41.52; Fe, 2.20; Cl, 1.39%. The infrared spectrum showed the bands at 1052, 1034 (shoulder), 941, 863, and 793 cm^{-1}, and the UV−vis spectrum in acetonitrile/dimethyl sulfoxide ($v/v = 7:3$) at 23 °C showed a broad O→Mo charge-transfer absorption band at 307 nm (ϵ 29000 M^{-1}cm^{-1}), characteristic of the α-Keggin structure. No signals were observed for the ^{31}P NMR spectrum in acetonitrile at 22 °C because of the presence of P−O−Fe^{3+} (paramagnetic species) bond in the polyoxometalate structure in agreement with the literature.[40,41]

The stoichiometric cesium salt of $PMo_{12}O_{40}^{3-}$ ($Cs_{3.0}PMo_{12}O_{40}$) was prepared with an aqueous solution of cesium carbonate and $H_3PMo_{12}O_{40}$ as follows.[22,23] Aqueous solution of cesium carbonate (67.5 cm^3, 0.08 mol dm^{-3}) was added dropwise to 60.0 cm^3 of aqueous solution of $H_3PMo_{12}O_{40}$ (0.06 mol dm^{-3}) at 50 °C. The resulting solution was evaporated to dryness at 50 °C and the powder sample was carefully collected. Elemental analysis for $Cs_{3.0}PMo_{12}O_{40}$: found (calcd) Cs, 17.92 (17.95); Mo, 51.83 (51.84); P, 1.21 (1.22). $Cs_{3.0}PMo_{12}O_{40}$ showed a sharp ^{31}P MAS NMR signal at −4.5 ppm.

Fe^{3+}(0.8−5.0 wt %)/$Cs_{3.0}PMo_{12}O_{40}$ catalysts were prepared by the impregnation of $Cs_{3.0}PMo_{12}O_{40}$ with aqueous solution of $Fe(NO_3)_3\cdot 9H_2O$. An iron content of 2.5 wt % corresponded to that in $Cs_{2.8}H_{1.2}[PMo_{11}\{Fe(H_2O)\}O_{39}]\cdot 6H_2O$. It was confirmed by IR and X-ray diffraction spectroscopy that the

(23) Mizuno, N.; Yahiro, H. *J. Phys. Chem. B.* **1998**, *102*, 437.
(24) Grasselli, R. K.; Burrington, J. D. *Adv. Catal.* **1981**, *30*, 133.
(25) Nelson, S. M. In *Comprehensive Coordination Chemistry;* Pergamon Press: Oxford, 1987; p 217.
(26) Powell, A. K. *Struct. Bonding* **1992**, *88*, 1. Holm, R. H.; Kennepohl, D.; Solomon, E. I. *Chem. Rev.* **1996**, *96*, 2239.
(27) Panov, G. Z.; Uriarte, K. A.; Rodkin, M. A.; Sobolev, V. I. *Catal. Today* **1998**, *41*, 365.
(28) Marturano, P.; Drozdová, L.; Kogelbauer, A.; Prins, R. *J. Catal.* **2000**, *192*, 236 and refs 1−3 therein.
(29) Cavani, F.; Etienne, E.; Favaro, M.; Galli, A.; Trifirò, F.; Hecquet, G. *Catal. Lett.* **1995**, *32*, 215. Cavani, F.; Trifirò, F. *Stud. Surf. Sci. Catal.* **1997**, *110*, 19.
(30) Langpape, M.; Millet, J.-M. M.; Ozkan, U. S.; Boudeulle, M. *J. Catal.* **1999**, *181*, 80.
(31) Hill, C. L.; Prosser-McCartha, C. M. *Coord. Chem. Rev.* **1995**, *143*, 407.
(32) Albonetti, S.; Cavani, F.; Trifirò, F. *Catal. Rev. Sci. Eng.* **1996**, *38*, 413.
(33) Neumann, R. *Prog. Inorg. Chem.* **1998**, *47*, 317.
(34) Pope, M. T. *Heteropoly and Isopoly Oxometalates;* Springer-Verlag: Berlin, 1983; p 93.
(35) Nomiya, K.; Sugaya, M.; Miwa, M. *Bull. Chem. Soc. Jpn.* **1979**, *52*, 3107.
(36) Rob van Veen, J. A.; Sudmeijer, O.; Emeis, C.; de Wit, H. *J. Chem. Soc., Dalton Trans.* **1986**, 1825.
(37) Combs-Walker, L. A.; Hill, C. L. *Inorg. Chem.* **1991**, *30*, 4016.
(38) Min, J.-S.; Misono, M.; Taguchi, A.; Mizuno, N. *Chem. Lett.* **2001**, 28.
(39) Zonnevijlle, F.; Tourné, C. M.; Tourné, G. F. *Inorg. Chem.* **1982**, *21*, 2751.
(40) Lyon, D. K.; Miller, W. K.; Novet, T.; Domaille, P. J.; Evitt, E.; Johnson, D. C.; Finke, R. G. *J. Am. Chem. Soc.* **1991**, *113*, 7209.
(41) Chang, X.; Chen, Q.; Duncan, D. C.; Lachicotte, R. J.; Hill, C. L. *Inorg. Chem.* **1997**, *36*, 4381.

α-Keggin structure of $PMo_{12}O_{40}^{3-}$ and the cubic structure (a = 11.8 Å) of $Cs_{3.0}PMo_{12}O_{40}$ were kept for Fe^{3+}(0.8−5.0 wt %)/$Cs_{3.0}PMo_{12}O_{40}$ catalysts.

Characterization of Solid $Cs_{2.8}H_{1.2}[PMo_{11}\{Fe(H_2O)\}O_{39}]\cdot 6H_2O$ and Fe^{3+}(2.5 wt %)/$Cs_{3.0}PMo_{12}O_{40}$. Spectroscopic measurements were carried out at room temperature unless otherwise stated. Infrared spectra in the range of 400−4000 cm^{-1} (KBr disks) were measured with a Paragon 1000PC spectrometer (Perkin-Elmer). UV−visible spectra were recorded on a Lambda 12 UV/VIS spectrometer (Perkin-Elmer). The powder X-ray diffraction (XRD) patterns were recorded on a powder X-ray diffractometer (Materials Analysis and Characterization, MXP[3]) with Cu Kα radiation. Thermogravimetric analyses (TGA) were carried out with a SSC/5200 thermal gravimetric analyzer (Seiko Instruments). A platinum basket was used as a sample holder and the ca. 20-mg sample was put into it. The TG/DTA profile was measured in an O_2 flow at a heating rate of 10 °C min^{-1}. The ESR spectra were recorded at X-band on a JEOL JES-RE1X spectrometer with 30−60-mg samples. For the quantitative measurements, the signal was doubly integrated and compared with that of $CuSO_4\cdot 5H_2O$ powder. MAS NMR spectra were measured with a Chemagnetics CMX-300 Infinity spectrometer operating at 7.05 T. The sample was set into a zirconia rotor (7.5-mm diam). ^{31}P (121 MHz) MAS NMR spectra were recorded using single-pulse excitation. The MAS rate was 3 kHz. $(NH_4)H_2PO_4$ (1.0 ppm) was used as an external standard.

The BET surface areas were measured with an ASAP 2000 (Micromeritics Instrument Co.). The BET surface area of $Cs_{2.8}H_{1.2}[PMo_{11}\{Fe(H_2O)\}O_{39}]\cdot 6H_2O$ evacuated at room temperature for 1 h was 146 $m^2\ g^{-1}$. After use for the oxidation reaction, the catalyst was evacuated at 200 °C for 1 h and then the surface area was measured again. Just before and after the catalytic reaction, the change of the surface area was within ±10%.

Reducibility of catalysts was measured by the temperature-programmed reduction with hydrogen (H_2-TPR). Samples (700 mg) were pretreated in an O_2 stream (60 mL min^{-1}) at 200 °C for 1 h. The reducing gas, 10% hydrogen in nitrogen, flowed over the sample at 30 °C until no H_2 uptake was observed, and then the sample was heated to 200 °C at a rate of 2 °C min^{-1}. The H_2 uptake and H_2O evolution were monitored with a quadrupole mass spectrometer. Mass numbers (m/z) of 2 and 18 were used for the detection of amounts of H_2 and H_2O, respectively.

Reaction of 2-Propanol. Catalytic reactions were carried out with a flow reactor (Pyrex tube, 10-mm i.d.) at 180 °C under atmospheric pressure. The feed gas consisted of 17 vol % of 2-propanol, 35 vol % of O_2, and N_2 balance. The total flow rate was 24 $cm^3\ min^{-1}$. All the flow lines were heated at 120 °C to prevent adsorption of 2-propanol and products. Prior to the reaction, 0.8 g of each catalyst was treated in an O_2 stream (48 $cm^3\ min^{-1}$) for 1 h at 200 °C. The gases at the outlet of the reactor were taken out intermittently with the aid of a sampler connected directly to the system and analyzed by a gas chromatograph with FFAP (1.0 m), Porapak-Q (4.0 m), and Molecular Sieve 5A (1.2 m) columns. Selectivity was a fraction of the sum of the products and calculated on the C_3(2-propanol)-basis. Carbon balance was more than 90%.

Results and Discussion

Structure of Solid $Cs_{2.8}H_{1.2}[PMo_{11}\{Fe(H_2O)\}O_{39}]\cdot 6H_2O$. The infrared spectrum showed bands at 1063, 1044 (shoulder) (ν(P−O)), 963 (ν(Mo=O), terminal), 858 (ν(Mo−O−M) (M = Mo, Fe), corner-sharing octahedra), and 787 cm^{-1} (ν(Mo−O−M), edge-sharing octahedra) characteristic of the α-Keggin structure, and was similar to that of the phenyltrimethylammonium salt. The splitting of ν(P−O) band results from the decrease in the symmetry of PO_4 tetrahedron caused by the Fe-substitution for Mo in the $PMo_{12}O_{40}^{3-}$ framework.[42] No ^{31}P MAS NMR signals were observed as was described for the solution ^{31}P MAS NMR spectrum of the phenyltrimethylammonium salt.

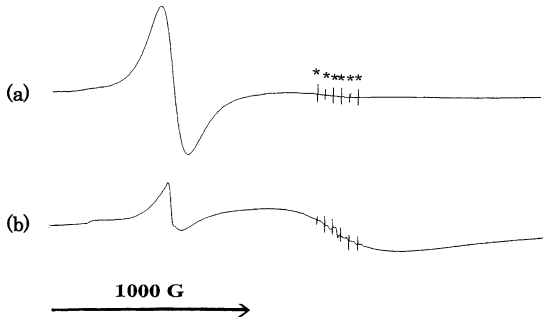

Figure 1. ESR spectra of (a) $Cs_{2.8}H_{1.2}[PMo_{11}\{Fe(H_2O)\}O_{39}]\cdot 6H_2O$; (b) Fe^{3+}(2.5 wt %)/$Cs_{3.0}PMo_{12}O_{40}$; *, signals of Mn marker.

ESR spectra of $Cs_{2.8}H_{1.2}[PMo_{11}\{Fe(H_2O)\}O_{39}]\cdot 6H_2O$ are shown in Figure 1a. The same signals were observed when the spectra were measured at −120 °C. An isotropic signal at g = 4.03 (ΔHpp = 290 G) was observed. It has been reported that high-spin Fe^{3+} incorporated in the silicotungstate structure with a distorted octahedral coordination gives an isotropic ESR signal (ΔHpp = ca. 170 G) at g = 4.12.[43] Therefore, the signal at g = 4.03 is assigned to high-spin Fe^{3+} incorporated in the polyoxometalate structure. The number of spins calculated with the ESR signal intensity was 3.0×10^{20} spins g^{-1} and fairly agreed with the amount of iron in $Cs_{2.8}H_{1.2}[PMo_{11}\{Fe(H_2O)\}O_{39}]\cdot 6H_2O$ (2.7×10^{20} atoms g^{-1}).

All the data for the solid cesium hydrogen salt show that the iron does not exist as countercations, but in the polyoxometalate.

States of Fe^{3+} in Fe^{3+}(2.5 wt %)/$Cs_{3.0}PMo_{12}O_{40}$. For Fe^{3+}(2.5 wt %)/$Cs_{3.0}PMo_{12}O_{40}$, no splitting of the IR band of ν(P−O) was observed, and a ^{31}P MAS NMR signal was observed at −4.5 ppm with the spinning sidebands. These facts show that the exchange of Fe^{3+} with Mo^{6+} does not proceed during the impregnation of Fe^{3+} on $Cs_{3.0}PMo_{12}O_{40}$. In addition, two ESR signals were observed for Fe^{3+}(2.5 wt %)/$Cs_{3.0}PMo_{12}O_{40}$ at g = 4.10 (ΔHpp = 180 G) and around g = 2.0 (ΔHpp = ca. 1400 G) as shown in Figure 1(b). In ref 44, the broad signals around g = 1.9−2.0 (ΔHpp = 1550 G) and g = 4.2 for $Fe_{0.85}H_{0.45}PMo_{12}O_{40}$ have been assigned to magnetically interacting Fe^{3+} with an octahedral coordination and countercation Fe^{3+} in relatively distorted octahedral sites,[45] respectively. Therefore, ESR data support the idea that the exchange of Fe^{3+} with Mo^{6+} does not proceed during the impregnation of Fe^{3+} on $Cs_{3.0}PMo_{12}O_{40}$.

Thermal Stability. The XRD pattern of $Cs_{2.8}H_{1.2}[PMo_{11}\{Fe(H_2O)\}O_{39}]\cdot 6H_2O$ showed signals at 2θ = 10.5, 18.3, 23.7, 26.1, and 30.2°, assignable to cubic phase with a = 11.8 Å. Not only these properties but also the

(42) Rocchiccioli-Deltcheff, C.; Thouvenot, R.; Frank, R. *Spectrochim. Acta A* **1976**, *32*, 587. Cadot, E.; Marchal, C.; Fournier, M.; Tézé, A.; Hervé, G. In *Polyoxometalate: From Platonic Solid to Antiretroviral Activity*; Pope, M. T., Müller, A., Eds.; Kluwer Academic: Dordrecht, The Netherlands, 1994; p 315.

(43) Rigny, P.; Pinsky, L.; Weulersse, J.-M. *C. R. Acad. Sci. Ser. C.* **1973**, *276*, 1223.

(44) Langpape, M.; Millet, J.-M. M. *Appl. Catal., A* **2000**, *200*, 89.

(45) The numbers of spins calculated with ESR signal intensities at g = 4.10 and 2.00 for Fe^{3+}(2.5 wt %)/$Cs_{3.0}PMo_{12}O_{40}$were 4.6×10^{19} and 4.4×10^{20} spins g^{-1}, respectively.

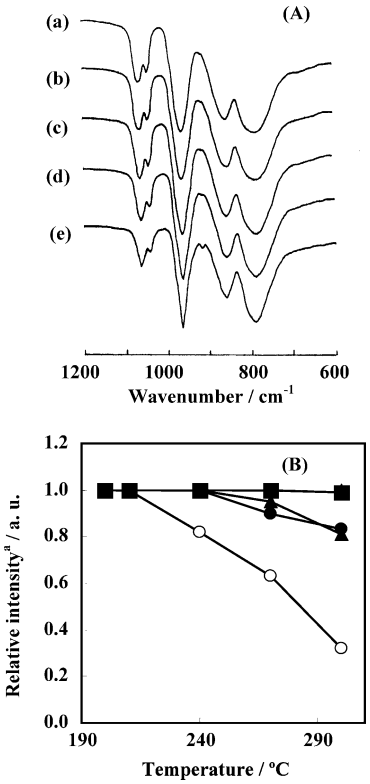

Figure 2. Changes in FT-IR spectra of $Cs_{2.8}H_{1.2}[PMo_{11}\{Fe(H_2O)\}O_{39}]\cdot 6H_2O$. (A) FT-IR spectra of $Cs_{2.8}H_{1.2}[PMo_{11}\{Fe(H_2O)\}O_{39}]\cdot 6H_2O$ treated in oxygen at (a) 25, (b) 200, (c) 240, (d) 270, and (e) 300 °C for 1 h. (B) IR band intensities; ●, ○, ■, ▲, and ■ represent IR band intensities at 1063, 1044, 963, 858, and 787 cm^{-1}, respectively. [a]Band intensities at 200 °C were taken as unity.

IR spectrum was not changed by the thermal treatment in O_2 below 210 °C (Figure 2A and 2B) and by the use for the catalytic reaction at 200 °C. The changes in the IR band intensities were plotted against the treatment temperature as shown in Figure 2B. The ESR spectra were hardly changed by the thermal treatment in O_2 below 210 °C in agreement with the IR data. By the treatment at and above 240 °C, the 1044-cm^{-1} band intensity was more decreased than that of the 1063-cm^{-1} band intensity. This may be caused by the elimination of the iron to form $PMo_{12}O_{40}^{3-}$. It was reported that the thermal treatment of $PVMo_{11}O_{40}^{4-}$ caused the elimination of vanadium to form $PMo_{12}O_{40}^{3-}$.[23,46]

The TG/DTA profile of $Cs_{2.8}H_{1.2}[PMo_{11}\{Fe(H_2O)\}O_{39}]\cdot 6H_2O$ showed two distinct endothermic peaks at 63 and 500 °C, assignable to desorption of 7.0 water molecules/anion and the decomposition of polyoxometalate, respectively. In addition, a weak endothermic peak was also observed around 210 °C. Taking IR and ESR data into account, the weak endothermic peak is probably attributable to the elimination of the substituted iron from the polyanion structure, in agreement with the decrease in the 1044-cm^{-1} band intensity in Figure 1B. These results show that $Cs_{2.8}H_{1.2}[PMo_{11}\{Fe(H_2O)\}O_{39}]\cdot 6H_2O$ is stable in O_2 or N_2 below 210 °C. Therefore, the reducibility and oxidation catalysis were carried out after $Cs_{2.8}H_{1.2}[PMo_{11}\{Fe(H_2O)\}O_{39}]\cdot 6H_2O$ was pretreated in O_2 at 200 °C for 1 h. The formula of the pretreated sample was estimated to be $Cs_{2.8}H_{1.2}PMo_{11}FeO_{39}$ and abbreviated as **I**. No peaks were observed around 210 °C for the TG/DTA profiles of Fe^{3+}(2.5 wt %)/$Cs_{3.0}PMo_{12}O_{40}$ and $Cs_{3.0}PMo_{12}O_{40}$.

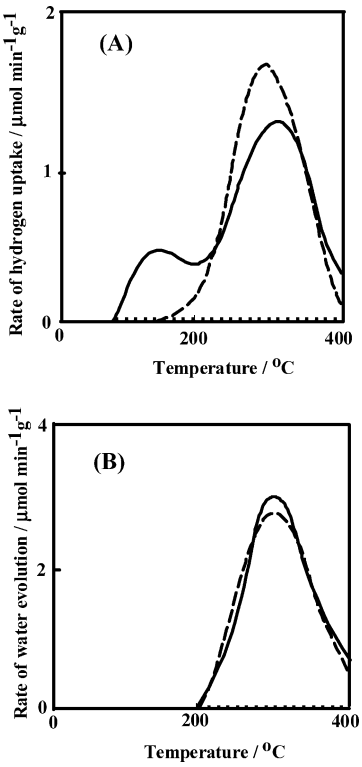

Figure 3. Profiles of hydrogen uptake (A) and water evolved (B) for H_2-TPR: solid line, **I**; dashed line, Fe^{3+}(2.5 wt %)/$Cs_{3.0}PMo_{12}O_{40}$; dotted line, $Cs_{3.0}PMo_{12}O_{40}$.

Reduction with H_2. It has been reported that rates of reduction with hydrogen can be used as a measure of oxidizing ability of catalysts for oxidative dehydrogenation reactions.[47] Figure 3a and b show profiles of hydrogen uptake and the water evolution, respectively.

$$PMo_{11}FeO_{39}^{4-} + x/2H_2 \rightarrow PMo_{11}FeO_{39}^{(4+x)-} + xH^+ \quad (1)$$

Below 200 °C no water was evolved for **I** while hydrogen uptake was observed. This shows the reduction of **I** with molecular hydrogen to form the reduced form and protons (eq 1), probably via the activation of H_2 by Fe^{3+}. Then water was evolved from 200 °C and the amount evolved below 400 °C was 0.16 $mmolg^{-1}$ corresponding to two times of hydrogen uptake (0.08 mmol g^{-1}).

For each catalyst no hydrogen uptake was observed at room temperature. The hydrogen uptake for **I** and Fe^{3+}(2.5 wt %)/$Cs_{3.0}PMo_{12}O_{40}$ catalysts started around 100 and 160 °C, respectively, whereas no hydrogen uptake was observed for $Cs_{3.0}PMo_{12}O_{40}$ below 400 °C (Figure 3A and Table 1). The amounts of hydrogen uptake below 180 °C were 11.0, 0.8, and 0 μmol g^{-1} for **I**, Fe^{3+}(2.5 wt %)/$Cs_{3.0}PMo_{12}O_{40}$, and $Cs_{3.0}PMo_{12}O_{40}$, respectively, as shown in Table 1. In addition, the color of **I** after the use for H_2-TPR up to 200 °C was slightly greenish yellow, whereas that of Fe^{3+}(2.5 wt %)/$Cs_{3.0}PMo_{12}O_{40}$ was almost yellow. Therefore, the reduc-

(46) Marchal-Roch, C.; Bayer, R.; Moisan, J. F.; Tézé, A.; Hervé, G. *Top. Catal.* **1996**, *3*, 407.

(47) Mizuno, N.; Watanabe, T.; Misono, M. *J. Catal.* **1990**, *123*, 157.

Table 1. Reducibility of Catalysts

catalyst	amount[a]	temp.[b]
I	11.0(80)	100
Fe^{3+}(1.3 wt %)/$Cs_{3.0}PMo_{12}O_{40}$	0.5(50)	170
Fe^{3+}(2.5 wt %)/$Cs_{3.0}PMo_{12}O_{40}$	0.8(80)	160
$Cs_{3.0}PMo_{12}O_{40}$	0	>400

[a] Total amount of hydrogen uptake below 180 °C in H_2-TPR (μmol g^{-1}). Numbers in the parentheses are total amounts of hydrogen uptake below 400 °C. [b] Starting temperature of hydrogen uptake (°C).

ibility decreased in the order of **I** > Fe^{3+}(2.5 wt %)/$Cs_{3.0}PMo_{12}O_{40}$ > Fe^{3+}(1.3 wt %)/$Cs_{3.0}PMo_{12}O_{40}$ > $Cs_{3.0}PMo_{12}O_{40} \approx 0$. The easiest reduction of **I** is probably related to the formation of $Fe^{3+}-O-Mo^{6+}$ bond in the polyanion framework and may be due to the cooperative reduction of Fe^{3+} coupled with that of Mo^{6+}, as has been reported in ref 48.

Effects of Iron Substitution on Oxidative Dehydrogenation of 2-Propanol. The reaction of 2-propanol was carried out with **I**, Fe^{3+}(0.8−5.0 wt %)/$Cs_{3.0}PMo_{12}O_{40}$, and $Cs_{3.0}PMo_{12}O_{40}$. The treatment in O_2 and the reactions of 2-propanol were performed below 200 °C to prevent the release of iron from the $PMo_{11}FeO_{39}^{4-}$ polyoxometalate as described in the previous section. In fact, no changes in IR (700−1100 cm^{-1}) and ESR spectra between as-prepared and spent $Cs_{2.8}H_{1.2}[PMo_{11}\{Fe(H_2O)\}O_{39}]\cdot 6H_2O$ were observed. For each experiment, hydrogen was hardly observed and the amount of water evolved was almost equal to the sum of the amount of O_2 consumed + the amount of propene produced + 0.5x (the amount of diisopropyl ether (DIPE) produced), showing that the dehydrogenation of 2-propanol to form hydrogen hardly proceeded.

The conversion and selectivity were determined after 2−5 h of reaction, when nearly steady-state conversion and selectivity were obtained for each catalyst, e.g., the conversions for **I** at 180 °C were 15, 14, 14, 14, and 14% at 1, 2, 3, 4, and 5 h, respectively. The products were acetone, propene, DIPE, and CO_2. Similar products were observed for the other catalysts used.

Table 2 summarizes the results for reactions of 2-propanol catalyzed by **I**, Fe^{3+}(2.5 wt %)/$Cs_{3.0}PMo_{12}O_{40}$, and $Cs_{3.0}PMo_{12}O_{40}$ at 180 °C. The reversible changes in conversion and selectivity for **I** were confirmed below the reaction temperature of 200 °C. The respective selectivities to acetone were 80, 38, and 16%, and **I** showed the highest selectivity, while the activities were close to one another. The selectivities to acetone for the reaction of 2-propanol catalyzed by Fe^{3+}(0.8−5.0 wt %)/$Cs_{3.0}PMo_{12}O_{40}$ were in the range of 22−38% and did not change much with the amounts of iron loaded. $Cs_{4.0}PMo_{11}FeO_{39}$ with no protons showed higher selectivity to acetone to 95%.[49]

The conversion linearly increased up to ca. 15% with W/F, where W is the weight of **I** and F is the flow rate of 2-propanol, as shown in Figure 4A. The selectivity to acetone, CO_2, propene, and DIPE almost unchanged with an increase in conversion, showing that successive

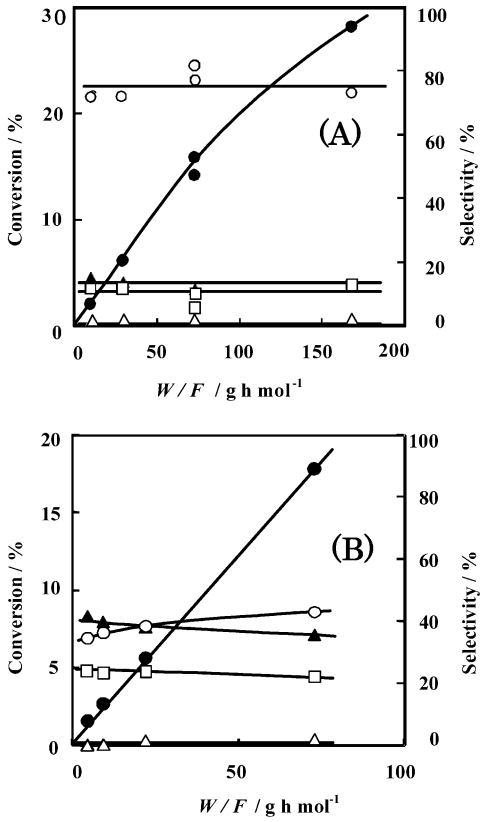

Figure 4. Changes in selectivity and conversion with W/F for the reaction of 2-propanol at 180 °C catalyzed by (A) **I** and (B) Fe(2.5 wt %)/$Cs_{3.0}PMo_{12}O_{40}$; ●, ○, ▲, □, and △ represent conversion of 2-propanol and selectivities to acetone, propene, DIPE, and CO_2, respectively.

reaction hardly proceeds. On the other hand, for Fe^{3+}(2.5 wt %)/$Cs_{3.0}PMo_{12}O_{40}$ the selectivity changed a little with the decrease in W/F to zero as shown in Figure 4B. The intrinsic catalytic activities at 180 °C evaluated by the slopes of conversion vs W/F lines for **I**, Fe^{3+}(2.5 wt %)/$Cs_{3.0}PMo_{12}O_{40}$, and $Cs_{3.0}PMo_{12}O_{40}$ were 2.4, 2.5, and 1.0 mmol g^{-1} h^{-1}, respectively. The selectivities to acetone extrapolated to 0% conversion for **I**, Fe^{3+}(2.5 wt %)/$Cs_{3.0}PMo_{12}O_{40}$, and $Cs_{3.0}PMo_{12}O_{40}$ were 76, 31, and 16%, respectively. It follows that the order of intrinsic activity for the oxidative dehydrogenation is **I** (rate, 1.8 mmol g^{-1} h^{-1}) > Fe^{3+}(2.5 wt %)/$Cs_{3.0}PMo_{12}O_{40}$ (0.8) > Fe^{3+}(1.3 wt %)/$Cs_{3.0}PMo_{12}O_{40}$ (0.6) > $Cs_{3.0}PMo_{12}O_{40}$ (0.1), showing that isolated Fe^{3+} in the $PMo_{11}O_{39}^{7-}$ polyoxometalate is more effective on the oxidative dehydrogenation than countercation Fe^{3+}. The selectivity to acetone started to decrease around 220 °C and was 59% at 300 °C, where Fe^{3+} was partly removed from the polyoxometalate, supporting the idea. The activation energies for 2-propanol conversion to acetone changed in the same order as shown in Table 2.

Kinetics and Mechanism. After the stationary state was attained in a flow experiment at 180 °C, the supply of oxygen was stopped. The concentration of oxygen quickly decreased and became lower than 0.01−0.03% within 5 min. After 30 min in the absence of oxygen, the conversion and selectivity to acetone were 9 and 76%, respectively. The conversion decreased while the selectivity to acetone remained almost unchanged. This suggests the progress of the reaction of 2-propanol with

(48) Keita, B.; Belhouari, A.; Nadjo, L.; Contant, R. *J. Electroanal. Chem.* **1998**, *442*, 49.

(49) The details for synthesis and characterization of $H_{4.0-x}Cs_xPMo_{11}FeO_{39}$ and the oxidation catalysis will be reported in due course.

Table 2. Reaction of 2-Propanol at 180 °C

catalyst	conv./%	selectivity/%				activation energy[a]
		acetone	propene	DIPE	CO_2	
I	14	80	10	8	2	39
Fe^{3+}(0.8 wt %)/$Cs_{3.0}PMo_{12}O_{40}$	21	22	37	35	0	
Fe^{3+}(1.3 wt %)/$Cs_{3.0}PMo_{12}O_{40}$	22	26	40	34	0	43
Fe^{3+}(2.5 wt %)/$Cs_{3.0}PMo_{12}O_{40}$	18	38	38	23	0	44
Fe^{3+}(5.0 wt %)/$Cs_{3.0}PMo_{12}O_{40}$	23	32	48	20	0	
$Cs_{3.0}PMo_{12}O_{40}$	6	16	32	52	0	45

[a] Activation energy for the acetone production (kJ mol^{-1}). In the range of reaction temperatures 176−200 °C, a good linear correlation between ln(rate) and 1/temp (K) was observed for each catalyst.

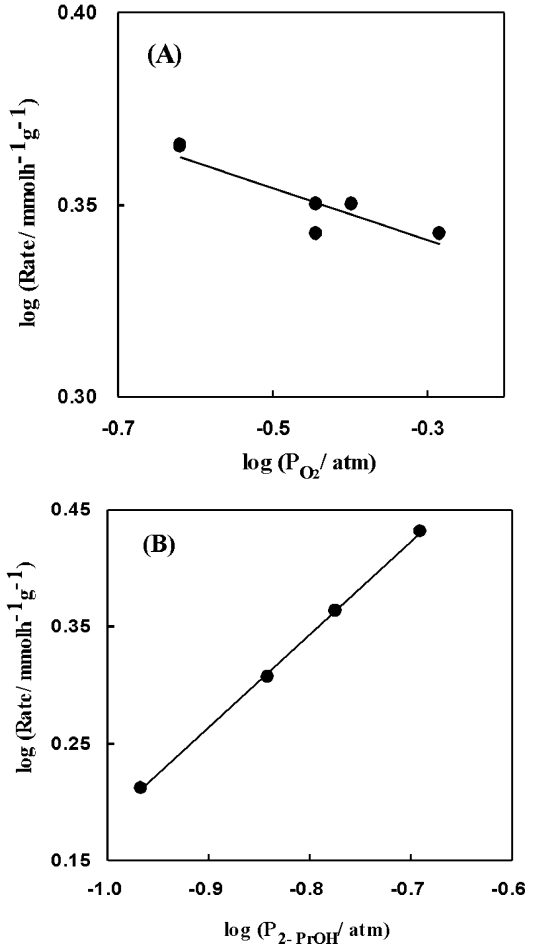

Figure 5. Dependencies of rates on partial pressures of (A) oxygen and (B) 2-propanol at 180 °C; catalyst, **I**.

I to produce acetone (eq 2).

$$PMo_{11}FeO_{39}^{4-} + x/2\ \text{2-propanol} \rightarrow PMo_{11}FeO_{39}^{(4+x)-} + x/2\ \text{acetone} + x\ H^+ \quad (2)$$

Dependencies of rates on the partial pressures of oxygen (0.25−0.52 atm) and 2-propanol (0.10 to 0.25 atm) for **I** are shown in Figure 5A and B, respectively. The slopes of log(rate) vs. log(P_{O2}) and log(rate) vs. log(P_{2-PrOH}) were −0.06 and 0.80, respectively, and the pressure dependencies were expressed by $-d[\text{2-PrOH}]/dt = k \cdot P_{2-PrOH}^{0.80} \cdot PO_2^{-0.06}$. The approximate first-order dependence of the rate on the pressure of 2-propanol and the almost zero-order dependence on the pressure of molecular oxygen suggest that the reduction of **I** with 2-propanol (eq 2) includes the rate-determining step and that the reoxidation of the reduced polyoxometalate with

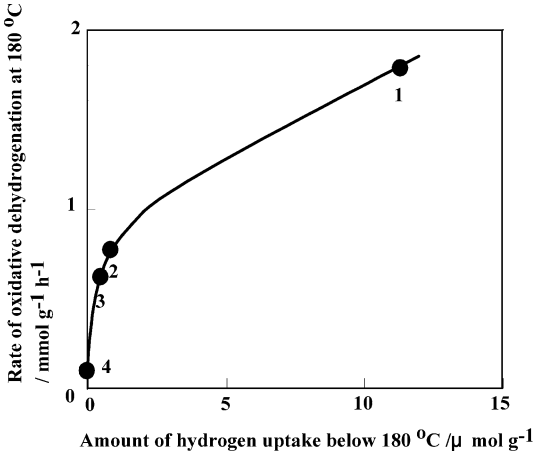

Figure 6. Correlation between intrinsic rate of oxidative dehydrogenation of 2-propanol and reducibility of catalysts: 1, **I**; 2, Fe(2.5 wt %)/$Cs_{3.0}PMo_{12}O_{40}$; 3, Fe(1.3 wt %)/$Cs_{3.0}PMo_{12}O_{40}$; and 4, $Cs_{3.0}PMo_{12}O_{40}$. Reducibility, see Table 1. Intrinsic rate of oxidative dehydrogenation of 2-propanol, (total rate obtained by the slope of W/F in Figure 6) × (%selectivity to acetone extrapolated to 0% conversion in Figure 5) × 10^{-2}.

molecular oxygen (eq 3) smoothly proceeds.

$$PMo_{11}FeO_{39}^{(4+x)-} + x\ H^+ + x/4\ O_2 \rightarrow PMo_{11}FeO_{39}^{4-} + x/2\ H_2O \quad (3)$$

When intrinsic rates of catalytic oxidative dehydrogention of 2-propanol were plotted against amounts of hydrogen uptake (i.e., noncatalytic reduction of catalyst), the rates increased with increase in reducibility of the catalysts as shown in Figure 6. The kinetic isotope effect (k_H/k_D) of 1.6−1.9 was observed for O_2/2-propanol-H_8 and O_2/2-propanol-D_8 in the temperature range of 180−200 °C. These facts suggest that the reduction of **I** with the β-hydrogen elimination from 2-propanol to form proton and reduced **I** is the rate-determining step in eq 2.

Conclusion

The mono-iron-substituted molybdophosphate, $PMo_{11}FeO_{39}$,$^{4-}$ was successfully synthesized and the crystal structure was determined as a phenyltrimethylammonium salt. The cesium hydrogen salt showed intrinsically higher activity for the oxidative dehydrogenation of 2-propanol to acetone compared with the iron-impregnated $Fe^{3+}/Cs_{3.0}PMo_{12}O_{40}$ and $Cs_{3.0}PMo_{12}O_{40}$ catalysts. It is demonstrated that the incorporation of iron into molybdophosphate framework much more enhances the catalytic performance for the oxidative dehydrogenation of 2-propanol than the conventionally

impregnated catalyst. The enhancement is probably due to an increase in reducibility (oxidizing ability) of the catalyst. The results offer an important strategy for development of new heterogeneous selective oxidation catalysts.

Acknowledgment. We acknowledge Prof. M. Misono (Kogakuin University), Prof. H. Yahiro (Ehime University), and Dr. S. Uchida (The University of Tokyo) for the encouragement of this work, discussion of ESR data, and solid state MAS NMR measurements, respectively. This work was supported in part by a Grant-in-Aid for Scientific Research from the Ministry of Education, Culture, Sports, Science and Technology of Japan and by the Core Research for Evolutional Science and Technology (CREST) program of Japan Science and Technology Corporation (JST).

Supporting Information Available: X-ray crystallographic file of $[C_6H_5(CH_3)_3N]_5[PMo_{11}\{Fe(Cl)\}O_{39}]\cdot 2CH_3CN$ (CIF), acidity of catalysts, IR spectrum of $[C_6H_5(CH_3)_3N]_5[PMo_{11}\{Fe(Cl)\}O_{39}]\cdot CH_3CN\cdot H_2O$, UV−vis spectrum of $[C_6H_5(CH_3)_3N]_5[PMo_{11}\{Fe(Cl)\}O_{39}]\cdot CH_3CN\cdot H_2O$, and TG/DTA profile of **I** (PDF). This material is available free of charge via the Internet at http://pubs.acs.org.

CM0348996